doi:10.1016/j.jmb.2011.05.003 J. Mol. Biol. (2011) 410, 477–487

Contents lists available at www.sciencedirect.com

Journal of Molecular Biology

journal homepage: http://ees.elsevier.com.jmb

Characterization of the Interaction of GABARAPL-1 with the LIR Motif of NBR1

Alexis Rozenknop[1,2], Vladimir V. Rogov[1,3], Natalia Yu. Rogova[1], Frank Löhr[1], Peter Güntert[1,4], Ivan Dikic[2,5] and Volker Dötsch[1]*

[1]*Institute of Biophysical Chemistry and Center for Biomolecular Magnetic Resonance, Goethe University, 60438 Frankfurt, Germany*
[2]*Institute of Biochemistry II, Goethe University Medical School, 60590 Frankfurt, Germany*
[3]*Institute of Protein Research, 142290 Pushchino, Russia*
[4]*Frankfurt Institute for Advanced Studies, Ruth-Moufang-Strasse 1, 60438 Frankfurt, Germany*
[5]*Frankfurt Institute for Molecular Life Sciences, Goethe University, 60438 Frankfurt, Germany*

Received 3 February 2011;
received in revised form
21 April 2011;
accepted 3 May 2011
Available online
18 May 2011

Edited by A. G. Palmer III

Keywords:
selective autophagy;
LIR;
GABARAP proteins;
LC3 proteins;
NBR1

Selective autophagy requires the specific segregation of targeted proteins into autophagosomes. The selectivity is mediated by autophagy receptors, such as p62 and NBR1, which can bind to autophagic effector proteins (Atg8 in yeast, MAP1LC3 protein family in mammals) anchored in the membrane of autophagosomes. Recognition of autophagy receptors by autophagy effectors takes place through an LC3 interaction region (LIR). The canonical LIR motif consists of a WXXL sequence, N-terminally preceded by negatively charged residues. The LIR motif of NBR1 presents differences to this classical LIR motif with a tyrosine residue and an isoleucine residue substituting the tryptophan residue and the leucine residue, respectively. We have determined the structure of the GABARAPL-1/NBR1-LIR complex and studied the influence of the different residues belonging to the LIR motif for the interaction with several mammalian autophagy modifiers (LC3B and GABARAPL-1). Our results indicate that the presence of a tryptophan residue in the LIR motif increases the binding affinity. Substitution by other aromatic amino acids or increasing the number of negatively charged residues at the N-terminus of the LIR motif, however, has little effect on the binding affinity due to enthalpy-entropy compensation. This indicates that different LIRs can interact with autophagy modifiers with unique binding properties.

*Corresponding author. E-mail address: vdoetsch@em.uni-frankfurt.de.

Abbreviations used: Atg, autophagy-related protein; GABARAPL-1, γ-aminobutyric acid receptor-associated protein-like 1; hp, hydrophobic pocket; HSQC, heteronuclear single quantum coherence; ITC, isothermal titration calorimetry; LIR, LC3 interacting region; MAP1LC3, light chain 3 of microtubule-associated protein 1; NBR1, neighbor of BRCA1 gene 1 protein; Nix, Nip-like protein x; NOE, nuclear Overhauser effect; PB1, Phox and Bem1p; RMSD, root-mean-square deviation; TROSY, transverse relaxation-optimized spectroscopy; Ub, ubiquitin.

Introduction

Autophagy is a highly conserved catabolic pathway used in cells to deliver cytosolic components to the lysosome for degradation. Disregulation of autophagy pathways leads to several diseases, including neurodegenerative disorders and cancer.[1–3] A key step of autophagy is the recognition and isolation of substrates, which are surrounded by the autophagosome, a double-membrane sack capable of fusing with the lysosome.[4,5]

In yeast, the formation of autophagosomes is directly related to the conjugation of Atg8 to

phosphatidylethanolamine on the autophagosome membrane by a multi-step mechanism that requires several enzymes.[6,7] Atg8 serves as an effector protein that binds to multivalent receptor proteins that can also interact with the substrate simultaneously through a different domain.[8] Several mammalian homologs of Atg8 that have been identified form the MAP1LC3 protein family,[9,10] which consists of two subgroups, the LC3 and GABARAP proteins that are involved in the elongation of the phagophore membrane and in the maturation of autophagosomes, respectively.[11] Similar to Atg8, they can be coupled reversibly to lipids by a three-step ubiquitin (Ub)-like conjugation system[12,13] and thus become anchored to the membrane of autophagosomes.[14–16]

Degradation of protein aggregates can be regulated by autophagy via ubiquitin-dependent signals.[17] The prototypic autophagy receptor protein p62[18,19] binds to ubiquitin or poly-ubiquitin signals,[20] a common modification of misfolded proteins, through a C-terminal UBA domain,[21] polymerizes via an N-terminal PB1 domain and acts as a transporter for ubiquitinated cargo. Moreover, p62 possesses a DDDWTHLS sequence motif that enables p62 to interact with members of the MAP1LC3 protein family[22] and is therefore called an LC3-interacting region (LIR).[23–25] It was proposed that this interaction links the ubiquitinated substrate that should be degraded to the autophagy modifiers in the autophagosome membrane. Originally, LIR sequences were defined as a WXXL motif but further studies showed that neither the tryptophan nor the leucine residues are strictly conserved and a more general definition of the LIR sequence should be ΘXXΓ where Θ and Γ are aromatic and hydrophobic residues, respectively. The presence of one or more acidic residues N-terminal to this sequence is preferred.[26] Here, we refer to the aromatic Θ residue as position 1 and to the hydrophobic Γ residue as position 4 (Fig. 1). In the structure of p62 in complex with LC3B,[24,25] the Θ and Γ residues interact with hydrophobic pockets on the surface of the autophagy effector. The first hydrophobic pocket, hp1, interacts with the aromatic Θ residue and is situated between the core of the protein, which adopts an ubiquitin-like fold, and an N-terminal extension consisting of two helices. The hydrophobic Γ residue binds to the hydrophobic pocket hp2 located on the surface of the ubiquitin-like core domain. An analogous binding mode involving the two hydrophobic pockets and a similar structure of the effector protein has been observed in the structure of GABARAP with calreticulin[27] and suggested for the interaction of GABARAP with clathrin heavy chain,[28] NSF[29] or Nix.[30]

Recently, the neighbor of BRCA1 gene 1 (NBR1) has been identified as an autophagy receptor that shares similar features with p62.[8,31] Most LIR sequences have tryptophan at position 1 and leucine at position 4, whereas the LIR domain of NBR1 contains tyrosine and isoleucine, respectively, which could influence the interaction with MAP1LC3 proteins.

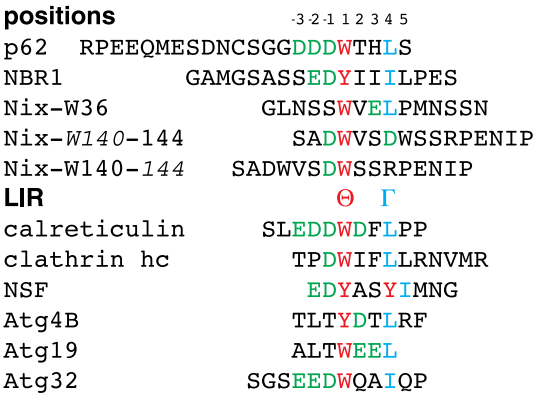

Fig. 1. Sequence alignments of LIR motifs in autophagy receptors (above the LIR motif) and enzymes modifying MAP1LC3 proteins as well as non-autophagic proteins (below the LIR motif). Aromatic residues corresponding to position 1 are marked in red, hydrophobic residues at position 4 in blue and negatively charged amino acids in green. All sequences are human except for Atg19 and Atg32, which are from *Saccharomyces cerevisiae*.

Binding of tryptophan-containing LIR domains to the LC3 and GABARAP proteins is structurally and functionally well characterized.[23–25,27,32–35] However, only a model of a complex of NSF[29] with GABARAP but no structure of a complex or a detailed interaction study of autophagy effector proteins with non-tryptophan LIR domains from autophagy receptors have been reported. The NBR1-LIR domain (YIIIL) has a more hydrophobic nature than the p62-LIR domain (WTHLS). This increased hydrophobicity could influence the interaction with MAP1LC3 effector proteins and might even lead to different or multiple orientations of the peptide in the binding site. To address this, we have studied the interaction of the NBR1-LIR domain with several human Atg8 family proteins, compared it to other LIR domains and determined the structure of its complex with GABARAPL-1. We also generated NBR1-LIR mutants with tryptophan or phenylalanine in place of the tyrosine in order to understand the importance of position 1 for the binding mode and we have introduced additional negatively charged amino acids N-terminal to the core LIR domain. The results show a tighter interaction between Atg8 family proteins and LIRs in the presence of tryptophan as well as the importance of the surrounding residues. The NMR structure of the GABARAPL-1–NBR1-LIR complex is the first example of the structure of a complex involving a non-tryptophan autophagy receptor–LIR domain.

Table 1. Thermodynamic parameters obtained by ITC

A. Interactions of LC3B with the LIR domains of different autophagy receptors

LC3B vs LIR	ΔH (kcal mol^{-1})	ΔS (cal mol^{-1} K^{-1})	ΔG (kcal mol^{-1})	K_d (μM)
p62	-10.5	-8.7	-8.0	1.5
Nix-W36	-2.7	+9.4	-5.5	91
Nix-W140/144	-2.8	+5.0	-4.3	670
NBR1	-4.4	+10.7	-7.6	2.9

B. GABARAPL-1 interaction with NBR1-LIR wild-type and mutants

GABARAPL-1 vs LIR	ΔH (kcal mol^{-1})	ΔS (cal mol^{-1} K^{-1})	ΔG (kcal mol^{-1})	K_d (μM)
NBR1	-4.1	+11.6	-7.6	3
NBR1_Y732W	-5.7	+10.3	-8.8	0.4
NBR1_Y732F	-6.8	+2.6	-7.6	2.9
NBR1_S729E	-4.8	+9.5	-7.6	2.7
NBR1_S728,729E	-5.5	+7.2	-7.7	2.4

Thermodynamic parameters obtained by ITC for the interactions of LC3B with the LIR domains of different autophagy receptors (A) and for GABARAPL-1 interaction with NBR1-LIR wild-type and mutants (B). All experiments were done at 25 °C. ΔH, ΔS and K_d values were measured with the assumption of a one-site model. Although statistical errors for all calculations were quite small (<3%), the uncertainty of the sample concentrations was ~5% (or more in the case of peptides containing no tryptophan or tyrosine residue). Therefore, a total error of 10% could be expected for all parameters.

Results

Interaction of LC3B with LIR domains

LC3B is the best studied mammalian Atg8 family member and its structure in the presence of p62 has been reported.[24,25] To compare the binding of different LIR sequences to MAP1LC3 proteins, we chose LC3B as an Atg8 model and its interaction with p62 as a reference. p62 is the prototypical LIR-containing protein with tryptophan and leucine as aromatic and hydrophobic amino acids and three aspartic acids as negatively charged residues.

In earlier work, we used NMR titration experiments and isothermal titration calorimetry (ITC) to characterize the interaction between the LIR domains of the autophagy receptors p62 and Nix with LC3B.[36] These experiments revealed that p62 interacts strongly with LC3B (K_d 1.5 μM), characterized by a slow exchange behavior in the NMR experiments and a strong negative binding enthalpy. Both Nix LIR domains (Nix-W36 and Nix–W140/144) interacted significantly more weakly (K_d 91 μM for Nix-W36 and 670 μM for Nix-W140/144) with a positive binding enthalpy and showed fast exchange between the bound and the free form in NMR titration experiments (Table 1).

To characterize the importance of the tryptophan residue at position 1 we compared binding of the non-tryptophan NBR1-LIR domain with those of the p62 and Nix LIR domains.

NMR titration experiments of the NBR1-LIR domain and LC3B showed a binding pattern similar to that of the p62–LIR interaction characterized by slow exchange. To obtain a more detailed analysis, we used ITC, which showed a dissociation constant (K_d) of 2.9 μM with a negative enthalpy (ΔH) of -4.4 kcal mol^{-1}, which is between the values for p62 and the Nix-LIR domains. These data indicate that the binding of side chains of the NBR1-LIR domain to the surface and the hydrophobic pockets on LC3B are less than optimal for p62. The less favorable binding enthalpy is, however, partially compensated by a positive entropy contribution (ΔS=10.7 cal mol^{-1} K^{-1}). p62 binding to LC3B is characterized by a strong negative entropy (ΔS=-8.7 cal mol^{-1} K^{-1}), which reduces the overall binding affinity. These differences in binding between NBR1 and the p62 LIR domains are likely to be caused by the more hydrophobic character and a reduced fitting of the aromatic residue to the hydrophobic pocket on LC3B.

Interaction of GABARAPL-1 with wild type and mutant NBR1-LIR

We wanted to further characterize the interaction of the NBR1-LIR domain with autophagy effector proteins by NMR investigations. However, the NMR spectra of a complex of LC3B with the NBR1-LIR domain revealed significant line-broadening of both peptide and protein resonances, making a detailed NMR investigation impossible. Therefore, we asked whether complex formation with other Atg8 family members would result in more favorable spectral characteristics. While all of the investigated family members (LC3A, LC3B, GABARAPL-1 and GABARAPL-2) exhibited broad lines due to exchange-broadening, the spectra of NBR1-LIR in complex with GABARAPL-1 showed the most favorable spectral characteristics, prompting us to further investigate this interaction. To investigate the role of the aromatic residue at position 1 we created a mutant form of NBR1-LIR in which the tyrosine was mutated to tryptophan,

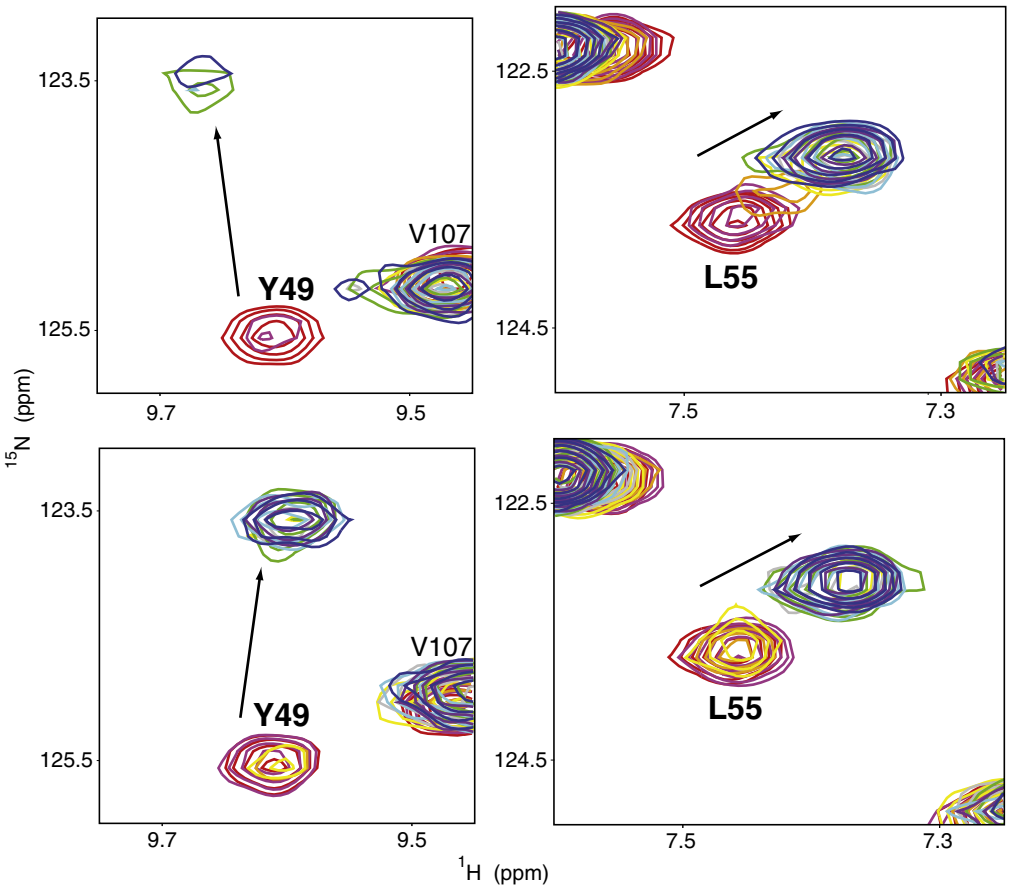

Fig. 2. GABARAPL-1 interaction with NBR1-LIR wild-type (top) and NBR1 LIR_Y732W (bottom). Overlay of representative regions (left for Y49 and right for L55) of [^{15}N, ^{1}H]-TROSY-HSQC spectra of GABARAPL-1 in presence of NBR1-LIR domains. Contours are presented in different colors corresponding to individual titration points (red as reference with GABARAPL-1 alone, magenta in presence of LIR domains at molar ratio 1:1/8, orange at molar ratio 1:1/4, yellow at molar ratio 1:1/2, gray at molar ratio 1:3/4, green at molar ratio 1:1, cyan at molar ratio 1:1.5, purple at molar ratio 1:2 and blue in presence of LIR domains at molar ratio 1:3). The data show that significant line broadening occurs with the wild-type sequence, characteristic of intermediate exchange while the mutant shows slow exchange behavior indicative of a stronger interaction.

which is more often observed at this position in LIR domains. NMR titration experiments of the ^{15}N-labeled GABARAPL-1 with both NBR1-LIR and the NBR1-LIR_Y732W mutant showed that the exchange-broadening of the tryptophan mutant was reduced compared to that of the wild type peptide, indicating a slower exchange between the bound and the free form (Fig. 2).

Indeed, measuring the binding affinity of GABARAPL-1 for NBR1-LIR and for the mutant by ITC revealed a stronger binding indicated by a reduction of the dissociation constant (K_d is 3 μM for the wild type domain and 0.4 μM for the mutant). The tighter binding of NBR1-LIR_Y732W is reflected in a more negative binding enthalpy contribution (ΔH=-5.7 kcal mol^{-1} *versus* ΔH=-4.1 kcal mol^{-1} for the wild type peptide). For both peptides, the binding entropy is large and positive (ΔS=10.3 cal mol^{-1} K^{-1} for NBR1-LIR_Y732W and ΔS=11.6 cal mol^{-1} K^{-1} for NBR1-LIR). The slightly reduced binding entropy for the mutant suggests that the tryptophan residue makes a tighter contact to GABARAPL-1, whereas there is more flexibility in the presence of the tyrosine residue (Table 1).

To further investigate the importance of the nature of the aromatic residue in position 1, we mutated the tyrosine residue in NBR1-LIR to phenylalanine. ITC experiments revealed a strong interaction with a very low binding entropy (ΔS=2.6 cal mol^{-1} K^{-1}), suggesting a tighter interaction that was reflected also by a more negative binding enthalpy (ΔH=-6.8 kcal mol^{-1}) relative to that of the wild type peptide.

In addition to the two important hydrophobic residues in positions 1 and 4 it has been shown that negatively charged amino acids located N-terminally to the aromatic residue participate in the

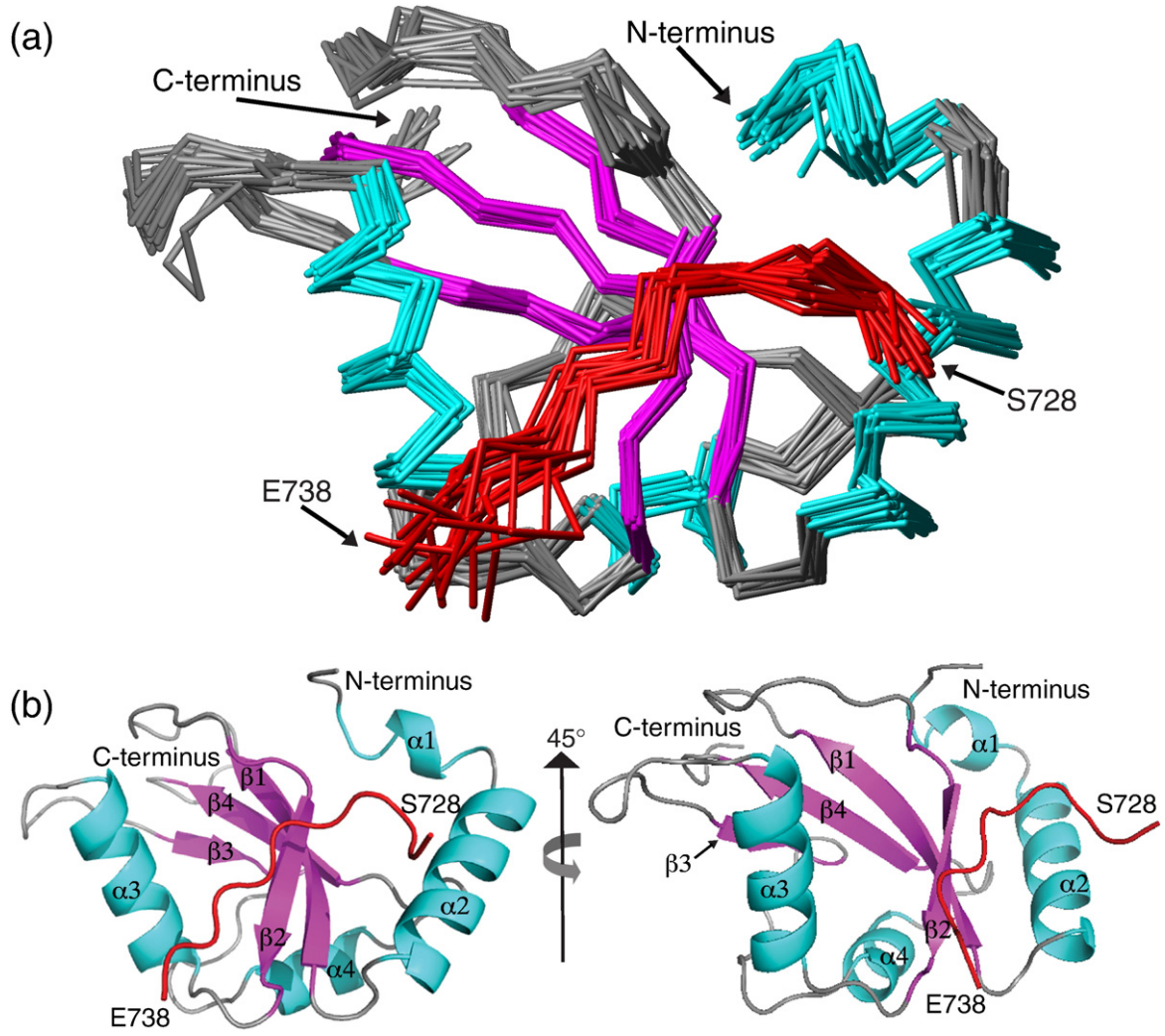

Fig. 3. NMR structure of the GABARAPL-1/NBR1-LIR complex**.** (a)**:** Overlay of the backbone atoms of the 20 energy-refined conformers of GABARAPL-1 in complex with NBR1-LIR. Loops are shown in gray, α-helices in cyan and β-strands in magenta. NBR1-LIR is colored in red. Residues 1-7 of GABARAPL-1 are disordered and were therefore excluded. Only the structured region of NBR1 (S728 to E738) is shown. (b): The mean structure of the complex is presented as a ribbon diagram in two orientations (the view on the right corresponds to a 45° rotation).

interaction.[24,25] Besides, the replacement of tryptophan with tyrosine, a further difference between p62 and NBR1 is the higher number of negatively charged amino acids N-terminal to the core LIR in p62 (three aspartic acid residues) relative to NBR1 (one aspartic acid residue and one glutamic acid residue). To investigate whether a higher number of negatively charged amino acids could compensate for the substitution of tryptophan with tyrosine, we extended the stretch of negatively charged amino acids directly N-terminal to Y732 in NBR1. Compared to the wild type, the mutation S729E resulted in a slightly increased affinity to GABARAPL-1 characterized by a more negative binding enthalpy (ΔH= -4.8 kcal mol^{-1}) and a decrease of the binding entropy (ΔS=9.5 cal mol^{-1} K^{-1}). These effects were further enhanced with the double mutant NBR1-LIR_S728,729E (ΔH=-5.5 kcal mol^{-1} and ΔS=7.2 cal mol^{-1} K^{-1}). In both cases, however, the overall effect was rather small owing to a remarkable compensation of enthalpy and entropy effects, resulting in K_d values that are not significantly different from the wild type peptide (2 – 3 μM). This mutational analysis showed that the strongest influence on the binding affinity is mediated by the presence or the absence of a tryptophan residue in position 1, making this position most important for explaining the differences in binding affinity between p62 and NBR1.

NMR structure of the GABARAPL-1/NBR1-LIR complex

The NMR titration experiments and the ITC data described above indicated that the replacement of

the tryptophan residue in position 1 with a tyrosine residue in the NBR1-LIR domain results in an increased flexibility in the interaction with Atg8 proteins. To further investigate this interaction, we solved the NMR structure of its complex with GABARAPL-1.

Detailed structural analysis of a complex requires the observation of NMR signals of the peptide in the presence of its effector protein. In titration experiments of ^{15}N-labeled NBR1-LIR with GABARAPL-1, we found disappearance of the amide resonances of amino acids D731, Y732, I733, I734, I735 and L736, all belonging to the core of the LIR motif. In the presence of a large excess of GABARAPL-1 (molar ratio of 1:10), these peaks reappeared but the sample was too unstable for further NMR experiments (results not shown). However, by performing titration experiments with ^{13}C-labeled NBR1-LIR, we were able to observe CH signals for all residues of the LIR domain at lower molar ratios. Focusing on the spectral region of the δ-methyl groups of isoleucine, we observed three overlapping peaks in the reference spectrum of the free peptide, which shifted significantly upon titration to three well distinguishable resonance positions. These NMR titration experiments indicated that a 1.5∼2.0 molar excess of one interaction partner is required to saturate the binding site and results in spectra of suitable quality for detailed structural analysis.

To obtain structural restraints for both partners, we recorded nuclear Overhauser effect spectra (NOESY) of complexes in which either GABARAPL-1 or the NBR1-LIR domain was ^{13}C/^{15}N-labeled in the presence of a 1.5 molar excess of the unlabeled interaction partner. Under these conditions, we were able to assign almost all resonances of GABARAPL-1 in the spectra (except for the N-terminal part near the small α-helix 1). Owing to line-broadening and protein concentration limitations (aggregation at ∼1.5 mM) classical half-filter experiments did not provide reliable intermolecular distance restraints. However, we were able to identify several intermolecular NOEs in 3D ^{13}C or ^{15}N-edited NOESY spectra. Under similar conditions, most of the side chain resonances of labeled NBR1 in complex with unlabeled GABARAPL-1 were observed and assigned and intra- as well as intermolecular NOEs were detected.

As expected, the 3D structure of GABARAPL-1 in the presence of the NBR1-LIR domain (represented in Fig. 3 and characterized in Table 2) is similar to the structure of other MAP1LC3 proteins.[37] The typical ubiquitin-like core ββαβαβ is preceded by two α-helices. These two N-terminal α-helices (α1, Q4 to D8; α2, F11 to K24) are the result of the positioning of a proline residue (P10) in the middle of a longer α-helix. The β-sheet domain is composed of four β-strands, two being parallel (β1, R28 to K35; β4, L105 to S110) and the other two are attached antiparallel (β2, K48 to P52; β3, F77 to V80). The two N-terminal helices close hydrophobic pocket hp1 formed by the convex side of the β-sheet. The other hydrophobic pocket, hp2, including the concave side is covered by α-helices α3 (V57 to R67) and α4 (M91 to D97) (Fig. 3). The structure of GABARAPL-1 in complex with the NBR1-LIR domain shows only small changes relative to the non-complexed crystal structure (PDB entry 2R2Q) with a backbone RMSD of 1.78 Å over the structured part (Q4 to S110).

Table 2. Structural statistics of the 20 energy-minimized conformers of GABARAPL 1/NBR1-LIR

A. Input restraint statistics	
Total number of meaningful distance restraints	1448 (84)[a]
Intraresidual ($i=j$)	207
Sequential ($\|i-j\|=1$)	436
Medium-range ($1 < \|i-j\| < 4$)	295 (46)[a]
Long-range ($\|i-j\| > 4$)	510 (38)[a]
Intermolecular	69 (8)[b]
Torsion angle restraints	203
B. Restraint violations in final ensemble (20 conformers)	
Distance restraint violations	
Number >0.1 Å	0
Maximal violations (Å)	0.09
RMS deviations from experimental restraints	
Distance restraints (Å)	0.0081 ± 0.0004
Angle restraints (deg)	0.55 ± 0.04
RMS deviations from idealized covalent geometry	
Bond lengths (Å)	0.0144 ± 0.0001
Bond angles (°)	1.730 ± 0.024
PROCHECK Ramachandran plot analysis	
Residues in most favoured regions (%)	85.3
Residues in addionally allowed regions (%)	13.3
Residues in generously allowed regions (%)	1.1
Residues in disallowed regions (%)	0.3
C. Structural precision[c] RMSD from ideal	
Backbone atoms N, C^{α}, C' (Å)	0.65 ± 0.11
All heavy atoms (Å)	1.21 ± 0.10

[a] The number of included H-bond restraints is indicated in parentheses.
[b] The number of manually assigned unambiguous intermolecular NOEs is indicated in parentheses.
[c] Values for the structured part (GABARAPL-1 residues 12–114, NBR1 residues 729–737).

In the complex, the LIR motif of the NBR1 peptide adopts an extended conformation and adds a β-strand to the central β-sheet of GABARAPL-1. The side chain of Y732 binds deep into the hp1 pocket and makes close contacts with E17, I21, P30, K46 and L50 with distances <4 Å. The hydrophobic pocket hp2 interacts with the side chain of I735 (Γ NBR1-LIR hydrophobic residue, position 4), with short distances to amino acids Y49, L50, V51 and P52 on one side of the pocket and L63, I64 and R67 on the other (Fig. 4). The other two hydrophobic amino acids, I733 and I734 at positions 2 and 3, are in contact with the surface of GABARAPL-1 (along strand β2). L736, the last hydrophobic residue at position 5, is in close proximity to hp2 but its side

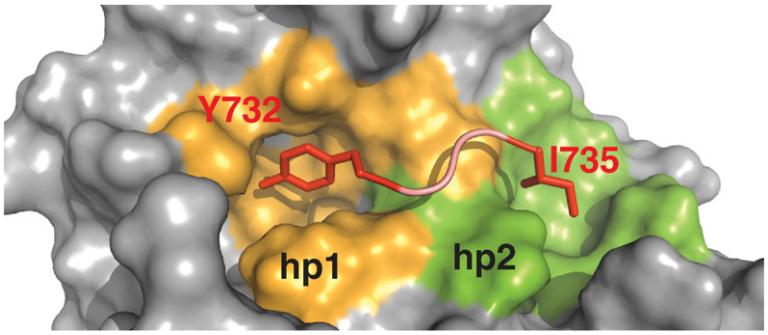

Fig. 4. LIR binding site of GABARAPL-1 in presence of the NBR1-LIR domain. The position of Y732 and I735 (red) within NBR1-LIR and their interaction with the hp1 (orange) and hp2 (green) on GABARAPL-1 (grey) are shown.

chain is oriented in a different direction and makes contact with V51 and P52. Finally, the two acidic amino acids E730 and D731 at positions -2 and -1 interact with the positively charged α-helix 2 (Fig. 5).

Discussion

The specificity of autophagy effector–receptor interactions is essential for selective degradation by autophagy. Initially, the LIR motif was characterized as a WXXL sequence; however, the discovery of additional proteins that act as autophagy receptors has led to a redefinition of its sequence.[26] For NBR1, it was shown that the YIII motif is crucial for its interaction with all members of the MAP1LC3 protein family.[31]

Here, we report the first NMR complex structure of a mammalian Atg8 homolog, GABARAPL-1, in the presence of a non-tryptophan receptor LIR domain, NBR1. The 3D structures of different MAP1LC3 proteins[38–44] have already been solved (mainly by X-ray crystallography) and show a high degree of structural similarity with an average backbone RMSD of 1.5 Å. In addition, the binding mode of peptides derived from different autophagy receptors is very similar to the structure of the GABARAPL–1/NBR1-LIR complex (RMSD 1.85 Å to the LC3B/p62 NMR structure (2K6Q)[25] over analogous secondary structure elements; RMSD 1.59 Å to the GABARAP/calreticulin X-ray structure (3DOW)[27] over the structured part E12-V114). Nevertheless, we observe differences. Careful analysis of the aromatic region of the NMR spectra revealed that the ε-protons of Y732 show two different peaks in the complex with GABARAPL-1, probably representing a major and a minor conformation. Unfortunately, the quality of the sample was not sufficient to observe specific NOEs for both conformations but only for the more intense resonance. However, during the structure calculation two different populations of the peptide with different positions of the tyrosine side chain in the hydrophobic pocket were consistent with the restraints, suggesting that potentially more than one conformation of the tyrosine side chain might exist (Fig. 6). A general tighter interaction involving a tryptophan residue in position 1 was confirmed by ITC experiments (LC3B/p62). To see whether the tyrosine residue indeed causes this flexibility, we mutated the tyrosine residue of the NBR1-LIR to a tryptophan residue to mimic more common LIR domains, such as p62, and we indeed observed a tighter interaction for this mutant. Replacing the tyrosine residue with a phenylalanine residue led to a more negative binding enthalpy but at the same time to a less positive binding entropy. Similarly,

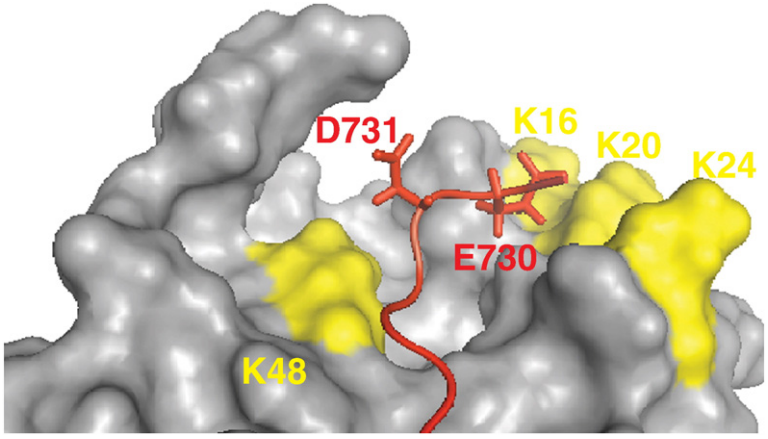

Fig. 5. Interaction of the acidic residues of NBR1-LIR with positively charged amino acids of GABARAPL-1. E730 and D731, located N-terminal to Y732 in NBR1-LIR, make close contacts with positively charged residues of GABARAPL-1, especially with residues in α-helix 2 (K16, K20 and K24).

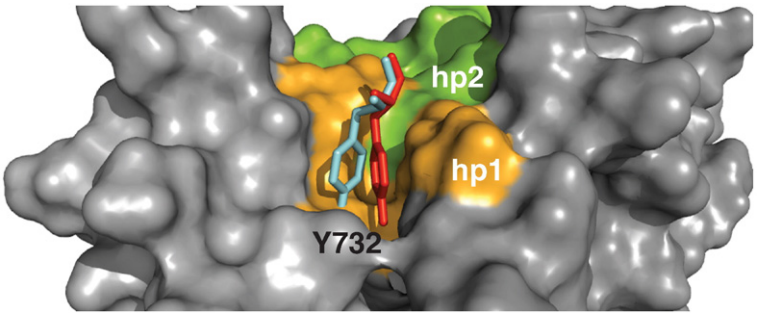

Fig. 6. Potential positions of the tyrosine residue of NBR1-LIR in the hp1 (orange) of GABARAPL-1. Both conformers are compatible with all NMR restraints and were observed in the structure calculation of the GABARAPL 1/NBR1-LIR complex.

introducing additional negatively charged amino acids also resulted in a more negative enthalpy but a less positive entropy relative to that of the wild type peptide. These results demonstrate that replacement of tryptophan at position 1 with other aromatic residues leads to a weaker interaction. Other mutations in the LIR domain, however, result in a remarkable enthalpy–entropy compensation allowing different sequences to interact with an overall similar binding affinity. This would allow autophagy effector proteins to interact with many different proteins with similar and moderate binding affinity, leading to a broad spectrum of interaction partners. Consequently, these effector proteins could interact with many more cellular binding partners than those currently known.

It has been shown that the type of amino acid at position 4 does not affect the interaction dramatically as long as the residue at this position provides sufficient hydrophobic surface.[33] In the NBR1-LIR domain, this position is occupied by an isoleucine residue and its side chain in our structure is oriented in hp2 in the same manner as the leucine residue in the LC3B/p62 complex.[24,25] The NBR1-LIR domain contains more hydrophobic residues than p62 at positions +2, +3 and +5 (isoleucine, isoleucine and leucine for threonine, histidine and serine). Such a hydrophobic track might lead to multiple binding modes or even competition of the individual amino acids for the hydrophobic pockets. The broad NMR resonances of amino acids in the core of the NBR1 LIR domain in complex with GABARAPL-1 show that conformational averaging indeed occurs, but at the same time did not allow us to characterize the different potential states in detail. The reappearance of NBR1 resonances at high molar ratios argues that a significant contribution to the observed line-broadening is due to intermediate exchange of the peptide between the bound and free state, but the observation of multiple resonances for Y732 suggests that, at least for some residues, multiple conformations in the bound state might occur. However, no multiple resonances or conformations during structure calculations have been observed for the isoleucine residues. The increased hydrophobic interaction throughout the entire NBR1-LIR domain might, however, compensate for the tight interaction lost by the replacement of the typical tryptophan residue with a tyrosine residue.

It has been shown that other amino acid positions besides the aromatic and the hydrophobic one affect the Atg8/LIR interaction significantly. Two LIR domains have been identified in Nix, a mitochondrial autophagy receptor[36,45,46] that is itself anchored in the mitochondrial membrane. Although both of them include a tryptophan residue, the interaction with Atg8 proteins is weaker than that for p62 and NBR1.[36] Like p62, Nix-W36 contains leucine as the hydrophobic amino acid at position 4 but binds weakly. The absence of negatively charged residues N-terminal to the aromatic residue reduces the interaction with the N-terminal residues of Atg8 proteins. Nix-W140/144 contains one acidic residue at position -1 (compared to three for p62 and two for NBR1) , most importantly, it does not have a hydrophobic residue at position 4. Consequently, our data show the weakest binding for Nix-W140/144. Thus, in addition to the presence of an aromatic amino acid buried in hp1, the hydrophobic interactions of the LIR motif with hp2 are essential and have to be complemented with electrostatic interactions mediated by negatively charged amino acids.

The specificity involved in autophagy receptor–effector interaction depends also on the effector proteins. Although only one Atg8 protein is present in yeast, eight orthologs belonging to two subfamilies (LC3 and GABARAP) have been characterized in mammals. Both subfamilies are essential for autophagosome formation but act differently; LC3 proteins are responsible for elongation, whereas GABARAP proteins are important for the maturation of autophagosomes.[11] Further detailed interaction studies of different autophagy receptor proteins with different Atg8 family members are necessary to understand specificity in this important process.

Materials and Methods

Cloning

PCR fragments encoding human MAP1LC3 proteins (LC3A, LC3B, GABARAPL-1 and GABARAPL-2) were cloned into a pETM-60 vector (EMBL) in which the NusA

leader was substituted with a modified ubiquitin between the NcoI and BamH1 sites. For the peptides (Nix-W36, amino acids 31–45; Nix-W140/144, 137–152; and NBR1-LIR, 722–739), the entire DNA sequences were obtained from MWG Bioscience and cloned into the same vector using the same restriction sites.

PCR-based, site-directed mutagenesis was used to introduce the point mutation to obtain Ub_NBR1-LIR_Y732W. NBR1-LIR_Y732F, NBR1-LIR_S729E and the double mutant NBR1-LIR_S728,729E were ordered from Peptide Specialty Laboratories (Germany).

Proteins and peptides

Plasmids encoding ubiquitin-fused proteins/peptides were transformed into the *Escherichia coli* NEB T7 Express strain. Bacteria were grown in LB medium for the expression of unlabeled proteins/peptides or in M9 medium for the expression of ^{15}N-labeled (1g/L $^{15}NH_4Cl$) and ^{13}C/^{15}N-labeled (1g/L $^{15}NH_4Cl$ and 2g/L ^{13}C-glucose) proteins/peptides. At an A_{600} ~1, IPTG was added to a final concentration of 1 mM to induce gene expression. After 3 h of expression at 37 °C, cells were harvested and suspended in 50 mM Tris, 250 mM NaCl, 5% (v/v) glycerol, pH 7.5 and lyzed in a French press. Cleared cell lysate (centrifugation for 30 min at 18,000 rpm) was loaded onto a Ni-NTA column, equilibrated with loading buffer (50 mM Tris, 250 mM NaCl, 1% glycerol and 10 mM imidazole, pH 7.7). The ubiquitin-fused protein/peptides constructs were eluted with a linear gradient of imidazole (10–400 mM). In the case of the proteins, the pure fractions were treated with tobacco etch virus protease and purified by size-exclusion chromatography in 50 mM sodium phosphate, 100 mM NaCl, pH 7.0.

Ub_NBR1-LIR samples for structure determination by NMR (unlabeled, ^{13}C/^{15}N-labeled and ^{13}C-labeled) were cleaved with tobacco etch virus protease and purified by size-exclusion chromatography in 10 mM ammonium acetate, pH 7.3. After lyophilization, NBR1-LIR was suspended in 50 mM sodium phosphate, 100 mM NaCl, pH 7.0. For NMR and ITC titrations, Ni-NTA elution fractions of Ub_NBR1-LIR and Ub_NBR1-LIR_Y732W were purified directly by size-exclusion chromatography in 50 mM sodium phosphate, 100 mM NaCl, pH 7.0.

Solid-phase synthesized and lyophilized peptides (p62-LIR: amino acids 321–342) were suspended in 50 mM sodium phosphate, 100 mM NaCl, pH 7.0.

Isothermal titration calorimetry (ITC)

ITC experiments were done at 25 °C using a VP-ITC calorimeter (MicroCal Inc., Northampton, MA, USA) and analyzed with the ITC-Origin software (MicroCal Inc.) based on the assumption of one-site binding reactions.

For LC3B experiments, 400 μM p62-LIR was titrated into 15 μM LC3B in 26 steps (10 μL/injection), 1.6 mM Nix-W36 into 80 μM LC3B, 2.0 mM Nix-W140/144 into 100 μM LC3B and 450 μM NBR1-LIR into 35 μM LC3B in 16 steps (15 μL/injection).

For GABARAPL-1 experiments, 350 μM Ub_NBR1-LIR wild type or mutants were titrated into 25 μM GABARAPL-1 in 26 steps (10 μL/injection).

NMR spectroscopy experiments

All NMR experiments done with Bruker Avance spectrometers operating at proton frequencies between 600 and 900 MHz. Spectra were analyzed with Sparky (UCSF). All experiments were done at 298 K.

NMR titration experiments

LC3B experiments with p62-LIR, Nix-W36 and Nix-W140/144 have been described.[36]

Unlabeled NBR1-LIR was added in an eight-step titration experiment to 120 μM ^{15}N-labeled LC3B solution to fivefold excess. ^{15}N-labeled GABARAPL-1 was concentrated to 100 μM and titration experiments were done by gradually adding unlabeled Ub_NBR1-LIR and Ub_NBR1-LIR_Y732W to a final molar ratio of 1:3. [^{15}N,^{1}H] transverse relaxation-optimized spectroscopy (TROSY)[47] spectra were recorded at each step.

Reverse titration experiments were done by gradually adding unlabeled GABARAPL-1 to ^{15}N-labeled NBR1-LIR and ^{13}C-labeled NBR1-LIR (1 mM concentration) to a final molar ratio of 1:1. After each addition of GABARAPL-1, [^{15}N,^{1}H] TROSY or [^{13}C,^{1}H] heteronuclear single quantum coherence (HSQC) spectra were recorded for ^{15}N_NBR1-LIR and ^{13}C_NBR1-LIR, respectively.

Resonances assignment

^{1}H, ^{15}N, $^{13}C^{\alpha}$ and $^{13}C^{\beta}$ resonances for LC3B and GABARAPL-1 proteins were obtained from individual HNCACB experiments with minor guidance by reported resonance assignments from BMRB entries 5958 and 5058 for LC3B and GABARAPL-1, respectively.

Backbone and side chain resonances for GABARAPL-1 in complex with the NBR1-LIR peptide were assigned using [^{15}N,^{1}H] TROSY versions of 3D HNCA, HNCACB, HNCO, HN(CA)CO, (H)CC(CO)NH-total correlation spectroscopy, TROSY-H(CCCO)NH-total correlation spectroscopy experiments. The assignment was supported and completed with ^{15}N-separated and ^{13}C-separated (for aliphatic and aromatic regions) NOESY-HSQC experiments. The same set of NMR experiments was used in addition to a 3D H(C)CH-total correlation spectroscopy experiment for the resonance assignment of NBR1-LIR in complex with GABARAPL-1.

For resonance assignment, the concentration of the labeled material was 0.6 mM and the unlabeled material was 0.9 mM.

Structure calculation

The CANDID module of CYANA 1.0.5[48] was applied to assign NOE signals in 3D ^{15}N and ^{13}C NOESY spectra and to calculate the structure of the GABARAPL-1/NBR1-LIR complex. In total, 4732 NOESY cross peaks (4140 from ^{13}C/^{15}N-labeled GABARAPL-1 and 592 from ^{13}C/^{15}N-labeled NBR1-LIR) together with 203 torsion angles restraints from TALOS[49] and 46 upper distance limits restraints for α-helical hydrogen bonds (identified as the consensus of the TALOS and CSI[50] programs) were used in the initial CYANA calculations. The 1364 meaningful distance restraints, 203 torsion angles restraints and 84 upper distance limits restraints for hydrogen bonds provided by the initial calculations were used to

calculate the final 20 (from 100) CYANA conformers with CYANA 3.0 (Table 2). These 20 final conformers with the lowest target function values were subjected to restrained energy minimization in explicit solvent against the AMBER force field[51] using the program OPALp.[52]

Protein Data Bank accession numbers

The atomic coordinates and NMR restraints of the GABARAPL-1/NBR1-LIR complex have been deposited in the Protein Data Bank with the accession number 2l8j. The chemical shift assignment is available in the Biological Magnetic Resonance Bank with the accession number 17412.

Acknowledgements

Financial support was obtained from the Center for Biomolecular Magnetic Resonance (BMRZ) and the Cluster of Excellence Frankfurt Macromolecular Complexes (CEF). P.G. acknowledges support by the Lichtenberg program of the Volkswagen Foundation. A.R. was funded by the Marie Curie ENDOCYTE training network.

Supplementary Data

Supplementary data to this article can be found online at doi:10.1016/j.jmb.2011.05.003

References

1. Mizushima, N., Levine, B., Cuervo, A. M. & Klionsky, D. J. (2008). Autophagy fights disease through cellular self-digestion. *Nature*, **451**, 1069–1075.
2. Levine, B. & Kroemer, G. (2008). Autophagy in the pathogenesis of disease. *Cell*, **132**, 27–42.
3. Dikic, I., Johansen, T. & Kirkin, V. (2010). Selective autophagy in cancer development and therapy. *Cancer Res.* **70**, 3431–3434.
4. Baba, M., Takeshige, K., Baba, N. & Ohsumi, Y. (1994). Ultrastructural analysis of the autophagic process in yeast: detection of autophagosomes and their characterization. *J. Cell Biol.* **124**, 903–913.
5. Xie, Z. & Klionsky, D. J. (2007). Autophagosome formation: core machinery and adaptations. *Nat. Cell Biol.* **9**, 1102–1109.
6. Ichimura, Y., Kirisako, T., Takao, T., Satomi, Y., Shimonishi, Y., Ishihara, N. *et al.* (2000). A ubiquitin-like system mediates protein lipidation. *Nature*, **408**, 488–492.
7. Suzuki, K. & Ohsumi, Y. (2007). Molecular machinery of autophagosome formation in yeast, *Saccharomyces cerevisiae*. *FEBS Lett.* **581**, 2156–2161.
8. Lamark, T., Kirkin, V., Dikic, I. & Johansen, T. (2009). NBR1 and p62 as cargo receptors for selective autophagy of ubiquitinated targets. *Cell Cycle*, **8**, 1986–1990.
9. He, H., Dang, Y., Dai, F., Guo, Z., Wu, J., She, X. *et al.* (2003). Post-translational modifications of three members of the human MAP1LC3 family and detection of a novel type of modification for MAP1LC3B. *J. Biol. Chem.* **278**, 29278–29787.
10. Xin, Y., Yu, L., Chen, Z., Zheng, L., Fu, Q. & Jiang, J. (2001). Cloning, expression patterns, and chromosome localization of three human and two mouse homologues of GABA(A) receptor-associated protein. *Genomics*, **74**, 408–413.
11. Weidberg, H., Shvets, E., Shpilka, T., Shimron, F., Shinder, V. & Elazar, Z. (2010). LC3 and GATE-16/GABARAP subfamilies are both essential yet act differently in autophagosome biogenesis. *EMBO J.* **29**, 1792–1802.
12. Tanida, I., Komatsu, M., Ueno, T. & Kominami, E. (2003). GATE-16 and GABARAP are authentic modifiers mediated by Apg7 and Apg3. *Biochem. Biophys. Res. Commun.* **300**, 637–644.
13. Tanida, I., Ueno, T. & Kominami, E. (2004). LC3 conjugation system in mammalian autophagy. *Int. J. Biochem. Cell Biol.* **36**, 2503–2518.
14. Kabeya, Y., Mizushima, N., Yamamoto, A., Oshitani-Okamoto, S., Ohsumi, Y. & Yoshimori, T. (2004). LC3, GABARAP and GATE16 localize to autophagosomal membrane depending on form-II formation. *J. Cell Sci.* **117**, 2805–2812.
15. Chakrama, F. Z., Seguin-Py, S., Le Grand, J. N., Fraichard, A., Delage-Mourroux, R., Despouy, G. *et al.* (2010). GABARAPL1 (GEC1) associates with autophagic vesicles. *Autophagy*, **6**, 495–505.
16. Kabeya, Y., Mizushima, N., Ueno, T., Yamamoto, A., Kirisako, T., Noda, T. *et al.* (2000). LC3, a mammalian homologue of yeast Apg8p, is localized in autophagosome membranes after processing. *EMBO J.* **19**, 5720–5728.
17. Kirkin, V., McEwan, D. G., Novak, I. & Dikic, I. (2009). A role for ubiquitin in selective autophagy. *Mol. Cell*, **34**, 259–269.
18. Bjorkoy, G., Lamark, T., Brech, A., Outzen, H., Perander, M., Overvatn, A. *et al.* (2005). p62/SQSTM1 forms protein aggregates degraded by autophagy and has a protective effect on huntingtin-induced cell death. *J. Cell Biol.* **171**, 603–614.
19. Bjorkoy, G., Lamark, T., Pankiv, S., Overvatn, A., Brech, A. & Johansen, T. (2009). Monitoring autophagic degradation of p62/SQSTM1. *Methods Enzymol.* **452**, 181–197.
20. Seibenhener, M. L., Babu, J. R., Geetha, T., Wong, H. C., Krishna, N. R. & Wooten, M. W. (2004). Sequestosome 1/p62 is a polyubiquitin chain binding protein involved in ubiquitin proteasome degradation. *Mol. Cell. Biol.* **24**, 8055–8068.
21. Vadlamudi, R. K., Joung, I., Strominger, J. L. & Shin, J. (1996). p62, a phosphotyrosine-independent ligand of the SH2 domain of p56lck, belongs to a new class of ubiquitin-binding proteins. *J. Biol. Chem.* **271**, 20235–20237.
22. Shvets, E., Fass, E., Scherz-Shouval, R. & Elazar, Z. (2008). The N-terminus and Phe52 residue of LC3 recruit p62/SQSTM1 into autophagosomes. *J. Cell Sci.* **121**, 2685–2695.
23. Pankiv, S., Clausen, T. H., Lamark, T., Brech, A., Bruun, J. A., Outzen, H. *et al.* (2007). p62/SQSTM1 binds directly to Atg8/LC3 to facilitate degradation of

ubiquitinated protein aggregates by autophagy. *J. Biol. Chem.* **282**, 24131–24145.
24. Ichimura, Y., Kumanomidou, T., Sou, Y. S., Mizushima, T., Ezaki, J., Ueno, T. *et al.* (2008). Structural basis for sorting mechanism of p62 in selective autophagy. *J. Biol. Chem*, **283**, 22847–22857.
25. Noda, N. N., Kumeta, H., Nakatogawa, H., Satoo, K., Adachi, W., Ishii, J. *et al.* (2008). Structural basis of target recognition by Atg8/LC3 during selective autophagy. *Genes Cells*, **13**, 1211–1218.
26. Noda, N. N., Ohsumi, Y. & Inagaki, F. (2010). Atg8-family interacting motif crucial for selective autophagy. *FEBS Lett.* **584**, 1379–1385.
27. Thielmann, Y., Weiergraber, O. H., Mohrluder, J. & Willbold, D. (2009). Structural framework of the GABARAP-calreticulin interface–implications for substrate binding to endoplasmic reticulum chaperones. *FEBS J.* **276**, 1140–1152.
28. Mohrlüder, J., Hoffmann, Y., Stangler, T., Hänel, K. & Willbold, D. (2007). Identification of clathrin heavy chain as a direct interaction partner for the gamma-aminobutyric acid type A receptor associated protein. *Biochemistry*, **46**, 14537–14543.
29. Thielmann, Y., Weiergräber, O. H., Ma, P., Schwarten, M., Mohrlüder, J. & Willbold, D. (2009). Comparative modeling of human NSF reveals a possible binding mode of GABARAP and GATE-16. *Proteins Struct. Funct. Bioinform.* **77**, 637–646.
30. Schwarten, M., Mohrluder, J., Ma, P., Stoldt, M., Thielmann, Y., Stangler, T. *et al.* (2009). Nix directly binds to GABARAP: a possible crosstalk between apoptosis and autophagy. *Autophagy*, **5**, 690–698.
31. Kirkin, V., Lamark, T., Sou, Y. S., Bjorkoy, G., Nunn, J. L., Bruun, J. A. *et al.* (2009). A role for NBR1 in autophagosomal degradation of ubiquitinated substrates. *Mol. Cell*, **33**, 505–516.
32. Waters, S., Marchbank, K., Solomon, E., Whitehouse, C. & Gautel, M. (2009). Interactions with LC3 and polyubiquitin chains link nbr1 to autophagic protein turnover. *FEBS Lett.* **583**, 1846–1852.
33. Weiergraber, O. H., Stangler, T., Thielmann, Y., Mohrluder, J., Wiesehan, K. & Willbold, D. (2008). Ligand binding mode of GABAA receptor-associated protein. *J. Mol. Biol.* **381**, 1320–1331.
34. Satoo, K., Noda, N. N., Kumeta, H., Fujioka, Y., Mizushima, N., Ohsumi, Y. & Inagaki, F. (2009). The structure of Atg4B-LC3 complex reveals the mechanism of LC3 processing and delipidation during autophagy. *EMBO J.* **28**, 1341–1350.
35. Mohrluder, J., Schwarten, M. & Willbold, D. (2009). Structure and potential function of gamma-aminobutyrate type A receptor-associated protein. *FEBS J.* **276**, 4989–5005.
36. Novak, I., Kirkin, V., McEwan, D. G., Zhang, J., Wild, P., Rozenknop, A. *et al.* (2009). Nix is a selective autophagy receptor for mitochondrial clearance. *EMBO Rep.* **11**, 45–51.
37. Noda, N. N., Ohsumi, Y. & Inagaki, F. (2009). ATG systems from the protein structural point of view. *Chem. Rev.* **109**, 1587–1598.
38. Coyle, J. E., Qamar, S., Rajashankar, K. R. & Nikolov, D. B. (2002). Structure of GABARAP in two conformations: implications for GABA(A) receptor localization and tubulin binding. *Neuron*, **33**, 63–74.
39. Kouno, T., Mizuguchi, M., Tanida, I., Ueno, T., Kanematsu, T., Mori, Y. *et al.* (2005). Solution structure of microtubule-associated protein light chain 3 and identification of its functional subdomains. *J. Biol. Chem.* **280**, 24610–24617.
40. Sugawara, K., Suzuki, N. N., Fujioka, Y., Mizushima, N., Ohsumi, Y. & Inagaki, F. (2004). The crystal structure of microtubule-associated protein light chain 3, a mammalian homologue of *Saccharomyces cerevisiae* Atg8. *Genes Cells*, **9**, 611–618.
41. Paz, Y., Elazar, Z. & Fass, D. (2000). Structure of GATE-16, membrane transport modulator and mammalian ortholog of autophagocytosis factor Aut7p. *J. Biol. Chem.* **275**, 25445–25450.
42. Bavro, V. N., Sola, M., Bracher, A., Kneussel, M., Betz, H. & Weissenhorn, W. (2002). Crystal structure of the GABA(A)-receptor-associated proteinGABARAP. *EMBO Rep.* **3**, 183–189.
43. Knight, D., Harris, R., McAlister, M. S., Phelan, J. P., Geddes, S., Moss, S. J. *et al.* (2002). The X-ray crystal structure and putative ligand-derived peptide binding properties of gamma-aminobutyric acid receptor type A receptor-associated protein. *J. Biol. Chem.* **277**, 5556–5561.
44. Stangler, T., Mayr, L. M. & Willbold, D. (2002). Solution structure of human GABA(A) receptor-associated protein GABARAP: implications for biological function and its regulation. *J. Biol. Chem.* **277**, 13363–13366.
45. Sandoval, H., Thiagarajan, P., Dasgupta, S. K., Schumacher, A., Prchal, J. T., Chen, M. & Wang, J. (2008). Essential role for Nix in autophagic maturation of erythroid cells. *Nature*, **454**, 232–235.
46. Schweers, R. L., Zhang, J., Randall, M. S., Loyd, M. R., Li, W., Dorsey, F. C. *et al.* (2007). NIX is required for programmed mitochondrial clearance during reticulocyte maturation. *Proc. Natl Acad. Sci. USA*, **104**, 19500–19505.
47. Pervushin, K., Riek, R., Wider, G. & Wüthrich, K. (1997). Attenuated T2 relaxation by mutual cancellation of dipole-dipole coupling and chemical shift anisotropy indicates an avenue to NMR structures of very large biological macromolecules in solution. *Proc. Natl Acad. Sci. USA*, **94**, 12366–12371.
48. Herrmann, T., Guntert, P. & Wuthrich, K. (2002). Protein NMR structure determination with automated NOE assignment using the new software CANDID and the torsion angle dynamics algorithm DYANA. *J. Mol. Biol.* **319**, 209–227.
49. Cornilescu, G., Delaglio, F. & Bax, A. (1999). Protein backbone angle restraints from searching a database for chemical shift and sequence homology. *J. Biomol. NMR*, **13**, 289–302.
50. Wishart, D. S. & Sykes, B. D. (1994). The ^{13}C chemical-shift index: a simple method for the identification of protein secondary structure using 13C chemical-shift data. *J. Biomol. NMR*, **4**, 171–180.
51. Ponder, J. W. & Case, D. A. (2003). Force fields for protein simulations. *Adv. Protein Chem.* **66**, 27–85.
52. Koradi, R., Billeter, M. & Guntert, P. (2000). Point-centered domain decomposition for parallel molecular dynamics simulation. *Comput. Phys. Commun.* **124**, 139–147.